

University of Groningen

Neuro-imaging of visual field defects

Boucard, Christine

IMPORTANT NOTE: You are advised to consult the publisher's version (publisher's PDF) if you wish to cite from it. Please check the document version below.

Document Version

Publisher's PDF, also known as Version of record

Publication date:

2006

[Link to publication in University of Groningen/UMCG research database](#)

Citation for published version (APA):

Boucard, C. (2006). *Neuro-imaging of visual field defects*. s.n.

Copyright

Other than for strictly personal use, it is not permitted to download or to forward/distribute the text or part of it without the consent of the author(s) and/or copyright holder(s), unless the work is under an open content license (like Creative Commons).

The publication may also be distributed here under the terms of Article 25fa of the Dutch Copyright Act, indicated by the "Taverne" license. More information can be found on the University of Groningen website: <https://www.rug.nl/library/open-access/self-archiving-pure/taverne-amendment>.

Take-down policy

If you believe that this document breaches copyright please contact us providing details, and we will remove access to the work immediately and investigate your claim.

Downloaded from the University of Groningen/UMCG research database (Pure): <http://www.rug.nl/research/portal>. For technical reasons the number of authors shown on this cover page is limited to 10 maximum.

CHAPTER 3

Visual field defects and the functional brain

Reorganisation in visual cortex associated with visual field defects?

Authors:

Christine C. Boucard

Nomdo M. Jansonius

Johanna M.M. Hooymans

Frans W. Cornelissen



Abstract

Due to the retinotopic organisation of visual cortex, visual field defects overlapping in both eyes prevent the stimulation of the corresponding cortical area. Prolonged absence of stimulation causes the brain to adapt its neuronal circuits. With the use of fMRI and common techniques, retinotopic maps of age-related macular degeneration (AMD) and glaucoma patients, as well as controls, were examined in an attempt to investigate whether cortical reorganization occurs in visual cortex as a result of acquired retinal visual field defects. From a clinical perspective, this question is highly significant as functional rehabilitation might be affected by cortical reorganisation.

We present here abnormal retinotopic maps in two cases of AMD. In one case, we argue that the atypical pattern was caused by extrafoveal fixation. In the other case, the pattern cannot be explained on the basis of a deviant fixation. Hence, some form of cortical reorganisation may have occurred in the right hemisphere of this subject. Further, no evident differences were found between the retinotopic maps of the glaucoma and control groups.

The assessment of cortical (re-)organisation in subjects with visual field defects is especially complicated as uncontrolled variables, such as extrafoveal fixation, can lead to abnormal retinotopic maps.

Introduction

Due to the retinotopic cortical organisation [1-4], when visual field defects occur in both eyes and overlap, a section of visual cortex no longer receives stimulation. Under prolonged absence of stimulation, the brain may respond adapting the cortical neuronal circuits [5,6].

Acquired visual field defects provide an exceptional opportunity to examine if the mature human visual cortex reorganises in response to abnormal visual experience. There is evidence that developmental visual disorders such as strabismus [7], amblyopia [8] and albinism [9] affect the structure of human occipital cortex. Previous research in our group also showed occipital cortical thinning in glaucoma (Boucard, 2006 a,b, submitted for publication). However, it has not been entirely settled whether long-term reorganization occurs in visual cortex during absence of visual input. In the human, while Sunness (2004) [10] reported a silent region in the visual cortex corresponding to the lesion projection zone in one subject known with age-related macular degeneration (AMD) subject, cortical reorganisation was found in two cases of AMD [11]. Abnormal retinotopic organisation was also found in rod monochromats, where the cones, and thus the fovea, are dysfunctional [12,13]. In a study using electrophysiology in macaque, after monocular retinal lesion, in spite of perceptual filling-in, no topographic reorganisation was measured in visual cortex [14]. Likely, in a recent fMRI paper, experimentally induced scotoma, including destruction of the RGC layer, in the peripheral visual field of macaque monkeys showed no sign of reorganisation even after seven months [15]. On the other hand, a number of studies reported reorganisation of receptive fields following induced retinal lesions in cats and monkeys [16-24], but the extend of RGC damage is unknown. There is a clear diversity of results in both animal and human research.

With our study, we aim to help to shed light on the diversity of findings in the current literature. By means of commonly used retinotopic techniques [1,25-27] in fMRI, we are examining retinotopic maps of AMD and glaucoma patients, as well as controls, in an

attempt to investigate the occurrence of cortical reorganisation in acquired retinal visual field defects. The question is highly relevant from a clinical point of view as cortical reorganisation might affect functional recovery after treatment of retinal disease.

Here, we present abnormal retinotopic maps in two cases of AMD. In the first case, the atypical pattern might have been generated by eccentric or extrafoveal fixation. However, in the second case, we did not find such an explanation for the abnormal retinotopic pattern. This may suggest that cortical reorganisation has occurred in one hemisphere. Furthermore, the retinotopic maps of the glaucoma and control groups showed no evident differences, suggesting most likely absence of cortical reorganisation.

Methods

Subjects

AMD1 is an 81-year-old male with visual acuity of 0.2 in the left eye and 0.08 in the right. AMD2 is a 68-year-old male with visual acuity of 0.8 in the left eye and 0.1 in the right. Both subjects are diagnosed with AMD since at least 3 years. They presented homonymous scotoma of at least 10 degrees diameter located in the foveal region. The glaucoma patients showed primarily large peripheral visual field defects heading towards fixation and were required to have homonymous scotoma of at least 10 degrees diameter located centrally in at least one quadrant, for a minimum of 3 years. In both groups, no other (neuro-) ophthalmic disease affecting the visual field was present. The control subjects have good visual acuity, no visual field defect, and are free of any ophthalmic, neurologic, or general health problem.

AMD is caused by accumulated waste products in the tissues underneath the macula that interfere with retinal metabolism and lead to retinal atrophy [28,29]. The disease causes centrally located visual field defects.

Materials and data acquisition

Visual fields were recorded using the Humphrey Field Analyzer (HFA; Carl Zeiss Meditec, Dublin, California, USA) running the 30-2 program Sita Fast.

High-resolution MRI was performed on a 3.0 Tesla Philips Intera (Best, The Netherlands). A “full” 3-D structural MRI was acquired on each subject using a T1 weighted magnetization sequence T1W/3D/TFE-2, 8 degrees flip angle, matrix size 256 • 256, yielding 170 slices, voxel size 0.9x0.9x1 mm, TR 8.70 ms. The scanning time was approximately of 10 min. In addition, a “partial” 3-D structural MRI was acquired on each subject using a T1 weighted magnetization sequence T1W/3D/TFE-2, 8 degrees flip angle, matrix size 256 • 256, yielding 108 slices, voxel size 0.8x0.8x2 mm, TR 8.70 ms. Scanning time was approximately 2 min. This “partial” anatomy was only performed in the occipital area and was used to align the functional data to the “full” anatomy.

Functional data was acquired using a T2*-weighted gradient-recalled echo planar imaging (EPI) sequence with a SENSE-head coil. Technical data for the measurements were TE 35 ms, TR 2000 ms, flip angle 79 degrees, 108 slices in one volume, voxel size 1.6x1.6x2.0 mm. The scan duration was 224 s. The field of view was 210 mm for all subjects. The functional scanning was only performed in the occipital area.

Stimulation

Stimuli were presented using a modified version of the RET software developed by the Vision Science and Technology Activities (VISTA) group at Stanford University (<http://white.stanford.edu/software/>). The software was developed in Matlab using routines of the Psychophysics Toolbox [30,31]; <http://psychtoolbox.org/>).

Stimuli were displayed with an Apple Macintosh iBook with 8-bit resolution per gun and projected onto a screen at the top end of the bore of the MR-scanner by means of a BARCO LCD-projector G300. Subjects viewed the stimuli through a mirror system supplied with the scanner. The viewing distance was 90 cm. Due to their central visual field defects, fixation in our group of visual field defects patients is peculiarly difficult. Therefore, in order to attain good fixation, the subjects were instructed to direct their

gaze towards the centre of a fixation cross that covered the whole screen. The cross changed colour at random intervals (between 1 and 3 s). To maintain the attention, subjects had to press a button as soon as they noted a colour change. Stable fixation was further controlled by means of an eye-tracker device (MR-Eyeview, SMI, Teltow, Germany) and its corresponding software IView which recorded eye movements during the whole experiment. All subjects maintained sufficiently accurate stable fixation.

Visual field maps were measured using an expanding ring and two (horizontal and vertical) bifield wedge-shaped conventional stimuli able to create travelling waves of neural activity in visual cortex [1,25,32,33]. Both stimuli consisted of drifting, achromatic (mean luminance ~ 50 cd/m²), dartboard contrast patterns (~ 90 % contrast) with contrast reversal rate of 8Hz. Stimuli were presented from the central fixation point to 9° of eccentricity during 6 cycles of 36 s each (approximately 3.5 minutes per run). Between each run, subjects could rest during 1 or 2 minutes.

Retinotopically organized visual areas share their borders at the vertical meridian representations. Therefore, boundaries between the different retinotopically organised areas were identified using bifield vertical wedge stimuli (figure 1). This permitted to localise primary visual cortex. Besides, a bifield horizontal wedge (figure 1) evoked activity in the centre of the different retinotopically organised areas in the hemisphere contralateral to the stimulation. Because the upper visual field is represented in the ventral cortical areas while the lower visual field in the dorsal areas, the ventral and dorsal edges of primary visual cortex could also be distinguished. Eccentricity was measured with the use of dynamic expanding rings (figure 2). As the ring moved from fovea to periphery, the activity at locations containing neurons with peripheral receptive fields is delayed relative to locations containing neurons with foveal receptive fields, creating a travelling wave of neural activity.

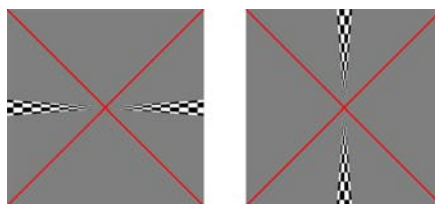


Figure 1. Horizontal and vertical bifield wedges.

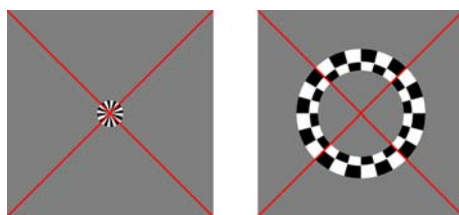


Figure 2. Two snapshots of the expanding ring pattern.

Data analysis

The first steps of data processing were performed using SPM (Statistical Parametric Mapping) software (Wellcome Department Imaging Neuroscience, London, UK; <http://www.fil.ion.ucl.ac.uk/spm/spm99.html>). To correct for the eventual motion during or between the functional runs, the EPI functional volumes were realigned to the first volume of the first run. Then, “partial” anatomy was co-registered to a functional volume. Next, using the VISTA toolbox, the “partial” anatomy was aligned to the “full” anatomy. In this way, the functional data spatially matches the “full” anatomy. Functional data was then averaged for every stimulus type (rings and wedges). The “full” anatomy was segmented separately by hemisphere. Finally, activations resulting from both rings and wedges were displayed on a flattened grey matter model of each hemisphere.

Using the wedge activations and their anatomical representations, we specified the location of V1. Next, the eccentricity information expressed by the rings within that area told us about the organisation of the representation of the visual fields in V1. Finally, the retinotopic map in V1 was assessed by visually examining the patterns.

Results

Figure 3 displays the representation of visual field eccentricity resulting from the expanding ring stimulation in a control subject (a), and two AMD patients (AMD1(b) and AMD2(c)).

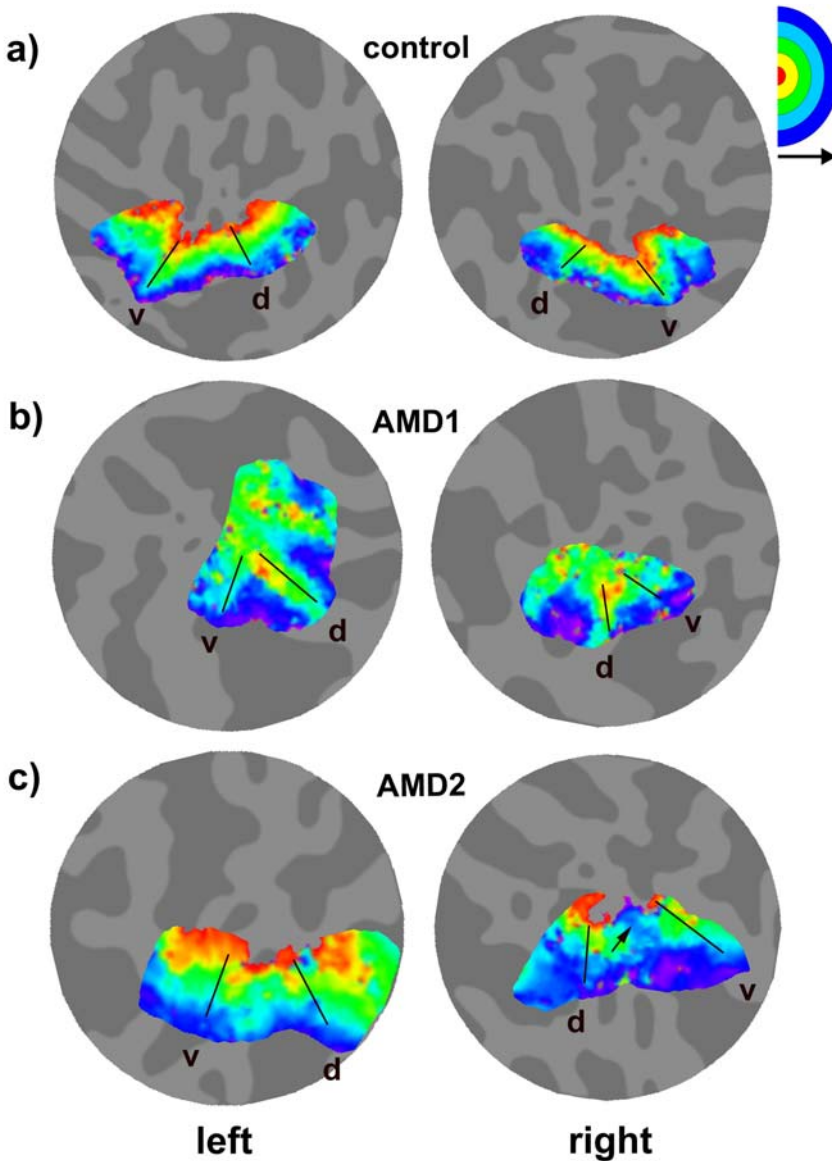


Figure 3. Retinotopic maps of the left and right hemispheres of a) control subject; b) patient AMD1; and c) patient AMD2 where the arrow points to the area of interest. The colours on the retinotopic map correspond to the location where the visual field was stimulated by the different rings (or stimulus phase). The icon on the right top indicates the relationship between colour and location where the visual field was stimulated (which corresponds to each phase of the stimulus). The black lines, drawn by hand along the activation corresponding to the vertical wedge, indicate the boundaries of V1. Letter “v” stands for ventral edge of V1, letter “d” for the dorsal edge.

A conventional retinotopic map is first shown in a). As it is expected by the retinotopic topography under which V1 is organised, each of the rings evoked activity preserving the eccentric order in which they were presented and without interruptions. This, of course, is based on the assumption that the fovea of both eyes were directed at the centre of the fixation cross.

When compared to the retinotopic map of a control subject, patients AMD1 and AMD2 exhibit abnormal retinotopic patterns.

In the case of AMD1 (b), in both hemispheres, the activation induced by the two most inner rings (red and yellow) is located on the dorsal edge of V1, while the central and ventral part of V1 responded to more outer rings (blue). The same pattern is repeated in the neighbouring retinotopic areas, such as V2. In this abnormal pattern, the activation seems to be shifted suggesting that the participant may have been using an extrafoveal part of the retina to fixate the center of the cross (figure 4).

AMD2 (c) presents a more or less conventional pattern in the left hemisphere, whereas in the right hemisphere the representation of the expanding rings is rather abnormal. Central fixation in this participant is confirmed by the conventional pattern in the left hemisphere. In the right hemisphere, under such central fixation, the expected continuous bands of yellow and green are interrupted by a section of blue that runs approximately through the middle of primary visual cortex. Hence, a section of cortex expected to be primarily responsive to the second and third inner rings (yellow and green) appears to have been activated by the outer rings (blue).

The retinotopic patterns from the glaucoma group did not show any clear difference from the maps from the control group, and are therefore not reproduced here.

Discussion

We here presented two atypical retinotopic maps of patients (AMD1 and AMD2) known with AMD, an acquired retinal visual field defect resulting in central scotoma.

First, we show how, after a careful analysis, the abnormal pattern found in AMD1 can be explained by eccentric or extrafoveal fixation. In the case of AMD2, we did not find other explanation than cortical reorganisation for the retinotopic pattern in the right hemisphere. Further, the retinotopic patterns from the glaucoma group did not show any clear difference from the maps from the control group.

In the case of AMD1, the pattern (figure 3b) can be explained by the fact that the subject did not fixate in the middle of the cross, as instructed, but opted for eccentric extrafoveal fixation. Fixation was additionally controlled by means of an eye-tracker device. However, the eye-tracker only controls for eye movements, reporting about the stability of the fixation, but fails in reporting about possible eccentric fixation. In the case of central scotoma, fixation is always an arduous task and complicates retinotopic measurements. As a strategy to overcome their foveal impairment, very often patients with central scotoma automatically adopt an extrafoveal preferred retinal locus (PRL) for fixation [34-36]. The schematic figure 4 shows the possible consequences of extrafoveal fixation along the vertical meridian in the upper visual field. In this case, the central stimulation (red) would fall onto the peripheral visual field. On the other hand, the foveal part of the visual field would be stimulated by a more peripheral phase (blue). Central and eccentric stimulation would no longer correspond with foveal and peripheral activation resulting in an atypical pattern of the central and eccentric phases, in the dorsal edge of V1. Such a retinotopic map can be seen in patient AMD1, where on the ventral part of V1, the blue colour prevails as a sign of peripheral stimulation. On its dorsal part, the whole visual field appears to be represented, but in a rather patchy manner. AMD1's retinotopic map is therefore consistent with extrafoveal fixation. No cortical reorganisation can be thus deduced from this atypical pattern.

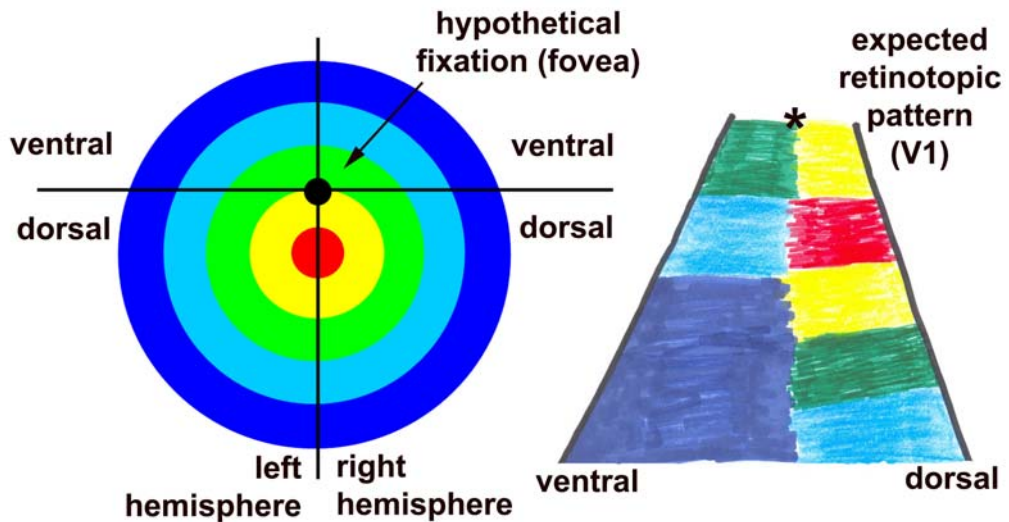


Figure 4. Schematic representation of the hypothetical retinotopic map resulting from eccentric or extrafoveal fixation along the vertical meridian in the upper visual field. On the left, the stimulation of the rings is represented by the different colours. The black point shows where the participant is hypothetically fixating with the fovea. The vertical and horizontal lines indicate how the visual field is represented in visual cortex. On the right, a drawing shows the expected retinotopic pattern within V1 in one hemisphere. The star (*) indicates the location of the foveal representation.

On the other hand, in the retinotopic map of patient AMD2 (figure 3c), the visual field is represented in a normal fashion, except for the central area (see arrow) in the right hemisphere. That area is normally expected to respond to parafoveal stimulation, as it holds projections from that area. However, here it reacted to the stimulation of the peripheral visual field (blue). The fact that the atypical pattern is only present in one hemisphere rejects the possibility of eccentric or extrafoveal fixation along the vertical meridian, since both hemispheres would show abnormal patterns in that case. Yet, the inner ring (red) representation in the pattern of the left hemisphere is located at the expected foveal area. The rest of the eccentricity map in the left hemisphere follows the conventional pattern, as well. It seems thus that in this case, fixation was centrally directed. Eccentric or extrafoveal fixation does not appear to be able to explain the observed retinopic pattern. Therefore, a possible explanation is that cortical

reorganisation may have occurred in the right hemisphere of AMD2. The causes of such a lateralisation are not clear to us. Manifestly, the complicate mechanisms behind cortical reorganisation still need to be investigated in depth.

A possible mechanism by which peripheral stimulation activates visual cortex in the location where the foveal and parafoveal representations are expected could be new intracortical horizontal connections formed by axonal sprouting. By such a mechanism, the visual input reaching active areas would eventually spread to deprived areas. Previous work in cats and monkeys assigned intracortical horizontal connections as the main factor accounting for the observed reorganisation after retinal lesions [19,37,38]. In our case, foveal and parafoveal silent cortical regions would attract connections from the unimpaired retinal periphery. The resulting retinotopic map would show invasion of central areas with peripheral ones.

In the case of glaucoma, there is progressive retinal ganglion cell (RGC) and optic nerve damage which leads to visual field loss starting peripherally and growing towards the fovea. As the retina presents additional peripheral loss, new connections would be more improbable to occur. On the other hand, there is substantial evidence linking cortical degeneration to glaucoma. Experimentally induced glaucoma in cats [39] and non-human primates [40] results in cell loss in visual cortex. Recent neuro-imaging work in our group also showed a lower grey matter concentration as a result of cortical thinning in the cortical lesion projection zone in human patients with glaucoma but not in AMD (Boucard et al., 2006a,b; submitted for publication). Degenerative changes in the visual cortex were also very recently reported in an autopsy examination of one glaucoma patient [41]. The fact that no obvious atypical patterns were seen in the retinotopic maps of our glaucoma group may suggest that cortical reorganisation does not occur in case of cortical degeneration. Perhaps, cortical atrophy prevents the formation of new horizontal connections.

The measurement of cortical organisation associated with abnormal visual fields is especially complicated because it is linked to a series of possible artefacts which can

lead to erroneous interpretations. Indeed, although finding atypical maps in the cortical projection zones can be a sign of cortical reorganisation, before linking an abnormal map to cortical reorganisation, one should primarily exclude any other possible explanation that could have originated the atypical pattern. Uncontrolled variables, such as extrafoveal fixation, can lead to abnormal retinotopic maps making the task of interpretation a very delicate one.

In the present study, the fact that we find only one possible case of cortical reorganisation implies caution in the conclusions and requires further investigation.

Finally, it should be mentioned that, because of the relative limited spatial resolution of fMRI, the technique we employ here only allows measuring the presence of large cortical reorganisation. Small changes in cortical organisation would most likely go unnoticed.

A better understanding of the relation between retinal visual field defects and functional changes in visual cortex may help understand disease symptoms as well as their progression. Moreover, cortical reorganisation may limit the efficacy of rehabilitation and training programs [42] as well as retinal prostheses aimed at restoring some degree of vision in the blind [43].

In order to understand the mechanisms behind cortical reorganisation, future retinotopic research should be directed towards the comparison of maps obtained from different disorders. For example, retinitis pigmentosa, which presents intact RGCs together with peripheral vision loss, would clarify the question if cortical reorganisation is related to intact RGC or to central location of scotoma. Likely, optical neuritis, where nerve damage is present, would also help bring additional insight to the issue.

Acknowledgement

C.C.B. is supported by an Ubbo Emmius grant from the University of Groningen, The Netherlands. The study was further supported by an equipment grant from the Prof.

Mulder foundation, Behavioural and Cognitive Neuroscience (BCN) school and the Medical Faculty of the University of Groningen. We would like to thank Ronald van den Berg and Just van Es for adapting the VISTA software, and Debora Zandbergen for her help in the experiments and data analysis.

References

1. Engel SA, Glover GH, Wandell BA. Retinotopic organization in human visual cortex and the spatial precision of functional MRI. *Cereb Cortex* 1997; 7:181-192.
2. Horton JC, Hoyt WF. The representation of the visual field in human striate cortex. A revision of the classic Holmes map. *Arch Ophthalmol* 1991; 109:816-824.
3. Inouye T. Die Sehstörungen bei Schussverletzungen der kortikalen Sehphäre nach Beobachtungen an Verwundeten der letzten japanischen Kriege. W Engelmann: Leipzig, 1909.
4. Tootell RB, Switkes E, Silverman MS, Hamilton SL. Functional anatomy of macaque striate cortex. II. Retinotopic organization. *J Neurosci* 1988; 8:1531-1568.
5. Johansson BB. Brain plasticity in health and disease. *Keio J Med* 2004; 53:231-246.
6. Merzenich MM, Nelson RJ, Stryker MP, Cynader MS, Schoppmann A, Zook JM. Somatosensory cortical map changes following digit amputation in adult monkeys. *J Comp Neurol* 1984; 224:591-605.
7. Chan ST, Tang KW, Lam KC, Chan LK, Mendola JD, Kwong KK. Neuroanatomy of adult strabismus: a voxel-based morphometric analysis of magnetic resonance structural scans. *Neuroimage* 2004; 22:986-994.
8. Mendola JD, Conner IP, Roy A, Chan ST, Schwartz TL, Odom JV, et al. Voxel-based analysis of MRI detects abnormal visual cortex in children and adults with amblyopia. *Hum Brain Mapp* 2005; 25:222-236.
9. von dem Hagen EA, Houston GC, Hoffmann MB, Jeffery G, Morland AB. Retinal abnormalities in human albinism translate into a reduction of grey matter in the occipital cortex. *Eur J Neurosci* 2005; 22:2475-2480.
10. Sunness JS, Liu T, Yantis S. Retinotopic mapping of the visual cortex using functional magnetic resonance imaging in a patient with central scotomas from atrophic macular degeneration. *Ophthalmology* 2004; 111:1595-1598.
11. Baker CI, Peli E, Knouf N, Kanwisher NG. Reorganization of visual processing in macular degeneration. *J Neurosci* 2005; 25:614-618.
12. Baseler HA, Brewer AA, Sharpe LT, Morland AB, Jagle H, Wandell BA. Reorganization of human cortical maps caused by inherited photoreceptor abnormalities. *Nat Neurosci* 2002; 5:364-370.
13. Morland AB, Baseler HA, Hoffmann MB, Sharpe LT, Wandell BA. Abnormal retinotopic representations in human visual cortex revealed by fMRI. *Acta Psychol (Amst)* 2001; 107:229-247.
14. Murakami I, Komatsu H, Kinoshita M. Perceptual filling-in at the scotoma following a monocular retinal lesion in the monkey. *Vis Neurosci* 1997; 14:89-101.
15. Smirnakis SM, Brewer AA, Schmid MC, Tolias AS, Schuz A, Augath M, et al. Lack of long-term cortical reorganization after macaque retinal lesions. *Nature* 2005; 435:300-307.
16. Calford MB, Wang C, Taglianetti V, Waleszczyk WJ, Burke W, Dreher B. Plasticity in adult cat visual cortex (area 17) following circumscribed monocular lesions of all retinal layers. *J Physiol* 2000; 524 Pt 2:587-602.
17. Chino YM. Adult plasticity in the visual system. *Can J Physiol Pharmacol* 1995; 73:1323-1338.
18. Chino YM, Kaas JH, Smith EL, 3rd, Langston AL, Cheng H. Rapid reorganization of cortical maps in adult cats following restricted deafferentation in retina. *Vision Res* 1992; 32:789-796.
19. Darian-Smith C, Gilbert CD. Axonal sprouting accompanies functional reorganization in adult cat striate cortex. *Nature* 1994; 368:737-740.
20. Gilbert CD. Adult cortical dynamics. *Physiol Rev* 1998; 78:467-485.
21. Gilbert CD, Wiesel TN. Receptive field dynamics in adult primary visual cortex. *Nature* 1992; 356:150-152.
22. Kaas JH. Neurobiology. How cortex reorganizes. *Nature* 1995; 375:735-736.
23. Kaas JH. Plasticity of sensory and motor maps in adult mammals. *Annu Rev Neurosci* 1991; 14:137-167.

24. Kaas JH. Sensory loss and cortical reorganization in mature primates. *Prog Brain Res* 2002; 138:167-176.
25. DeYoe EA, Carman GJ, Bandettini P, Glickman S, Wieser J, Cox R, et al. Mapping striate and extrastriate visual areas in human cerebral cortex. *Proc Natl Acad Sci U S A* 1996; 93:2382-2386.
26. Slotnick SD, Yantis S. Efficient acquisition of human retinotopic maps. *Hum Brain Mapp* 2003; 18:22-29.
27. Warnking J, Dojat M, Guerin-Dugue A, Delon-Martin C, Olympieff S, Richard N, et al. fMRI retinotopic mapping--step by step. *Neuroimage* 2002; 17:1665-1683.
28. Holz FG, Pauleikhoff D, Klein R, Bird AC. Pathogenesis of lesions in late age-related macular disease. *Am J Ophthalmol* 2004; 137:504-510.
29. Zarbin MA. Current concepts in the pathogenesis of age-related macular degeneration. *Arch Ophthalmol* 2004; 122:598-614.
30. Brainard DH. The Psychophysics Toolbox. *Spat Vis* 1997; 10:433-436.
31. Pelli DG. The VideoToolbox software for visual psychophysics: transforming numbers into movies. *Spat Vis* 1997; 10:437-442.
32. Engel SA, Rumelhart DE, Wandell BA, Lee AT, Glover GH, Chichilnisky EJ, et al. fMRI of human visual cortex. *Nature* 1994; 369:525.
33. Sereno MI, Dale AM, Reppas JB, Kwong KK, Belliveau JW, Brady TJ, et al. Borders of multiple visual areas in humans revealed by functional magnetic resonance imaging. *Science* 1995; 268:889-893.
34. Cheung SH, Legge GE. Functional and cortical adaptations to central vision loss. *Vis Neurosci* 2005; 22:187-201.
35. Varsori M, Perez-Fornos A, Safran AB, Whatham AR. Development of a viewing strategy during adaptation to an artificial central scotoma. *Vision Res* 2004; 44:2691-2705.
36. Sunness JS, Applegate CA, Haselwood D, Rubin GS. Fixation patterns and reading rates in eyes with central scotomas from advanced atrophic age-related macular degeneration and Stargardt disease. *Ophthalmology* 1996; 103:1458-1466.
37. Das A, Gilbert CD. Receptive field expansion in adult visual cortex is linked to dynamic changes in strength of cortical connections. *J Neurophysiol* 1995; 74:779-792.
38. Obata S, Obata J, Das A, Gilbert CD. Molecular correlates of topographic reorganization in primary visual cortex following retinal lesions. *Cereb Cortex* 1999; 9:238-248.
39. Chen X, Sun C, Huang L, Shou T. Selective loss of orientation column maps in visual cortex during brief elevation of intraocular pressure. *Invest Ophthalmol Vis Sci* 2003; 44:435-441.
40. Yucl YH, Zhang Q, Weinreb RN, Kaufman PL, Gupta N. Effects of retinal ganglion cell loss on magno-, parvo-, koniocellular pathways in the lateral geniculate nucleus and visual cortex in glaucoma. *Prog Retin Eye Res* 2003; 22:465-481.
41. Gupta N, Ang LC, Noel de Tilly L, Bidaisee L, Yucl YH. Human Glaucoma and Neural Degeneration in the Intra-cranial Optic Nerve, Lateral Geniculate Nucleus and Visual Cortex of the Brain. *Br J Ophthalmol* 2006.
42. Safran AB, Landis T. Plasticity in the adult visual cortex: implications for the diagnosis of visual field defects and visual rehabilitation. *Curr Opin Ophthalmol* 1996; 7:53-64.
43. Hossain P, Seetho IW, Browning AC, Amoaku WM. Artificial means for restoring vision. *Brmj* 2005; 330:30-3

